ELSEVIER

Physica A 312 (2002) 539–564

PHYSICA A

www.elsevier.com/locate/physa

Stock market dynamics

M.S. Baptista *, I.L. Caldas

Instituto de Física, Universidade de São Paulo, C.P. 66318, CEP 05315-970 São Paulo, S.P., Brazil

Received 2 January 2002

Abstract

We elucidate on several empirical statistical observations of stock market returns. Moreover, we find that these properties are recurrent and are also present in invariant measures of low-dimensional dynamical systems. Thus, we propose that the returns are modeled by the first Poincaré return time of a low-dimensional chaotic trajectory. This modeling, which captures the recurrent properties of the return fluctuations, is able to predict well the evolution of the observed statistical quantities. In addition, it explains the reason for which stocks present simultaneously dynamical properties and high uncertainties. In our analysis, we use data from the S&P 500 index and the Brazilian stock Telebrás.

PACS: 00.05.45.Gg; 00.05.45.Tp; 80.89.90.+n

Keywords: Chaos; Econophysics; Stock market; Dynamics; Modeling

1. Introduction

It is clear that the return distributions of stock market indexes does not have a Gaussian shape as proposed in Ref. [1], mainly due to the pronounced tail of these distributions. In Ref. [2] it is shown that the distribution of the fluctuations in cotton price is a stable Lévy distribution. However, due to the fact that the stable Lévy distribution has infinite variance, it does not fit well the decay of the distribution tail of the return indexes. The fact is that the asymptotic behavior of the return distribution shows faster decay than the one predicted by a Lévy distribution. Recently, a truncated unstable Lévy distribution, a Lévy distribution in the central part followed by an approximately exponential truncation, was proposed to describe the distribution of the return [3–5].

* Corresponding author. Tel.: +55-11-3091-7070; fax: +55-11-3091-6749.
E-mail address: murilo@if.usp.br (M.S. Baptista).

0378-4371/02/$ - see front matter
PII: S0378-4371(02)00847-6

Although a truncated Lévy distribution fits a return distribution, its tails follow a power-law asymptotic behavior, characterized by an exponent $\alpha \approx 3$, well outside the condition required for the Levy distribution stability ($0 < \alpha < 2$), as reported in Ref. [6].

Therefore, besides the relevant progress achieved in the statistical description of these fluctuations, a complete description of the return distributions has not been given in the previous works.

In recent works we showed that the return of the S&P 500 index has a Poisson-like distribution [7,8]. In agreement with this findings, in Ref. [9] the distribution of the increments of the British Pound/U.S.$ time series was found to decay as an exponential, a process whose distribution is a Poisson. Moreover, the observed Poisson-like distribution is equivalent to a Poisson-like distribution of the first Poincaré return time of a low-dimensional deterministic system. The first Poincaré return time measures the time a chaotic trajectory takes to return to a given reference interval in phase space.

One of the purposes of this work is to show that the distribution of the return of a stock index is the same for the recurrent time, i.e., the time the return takes to return to a specified interval of values. Furthermore, the other statistical properties of these two fluctuations can be simulated by measures of the first Poincaré return time of a low-dimensional trajectory. This equivalence, between the fluctuations of the return and a measure typical of chaotic dynamical systems, suggests that the stock market is dynamically recurrent, that is, there is a dynamical process ruling out the stock oscillations.

The use of dynamical tools, as the first Poincaré return time, can explain many empirical observations, described in the next section, for the return of a stock index [6,9,10]. In particular, the reason for the preservation, for long time scales, of the return distribution functional form. The model also describes very well how the average time intervals in which high return values occur (rare events) is related with the width of the return distribution (proportional to what is called volatility).

With the proposed procedure we explain properties and scales of the distributions for the return and the recurrent time of the S&P index and the Brazilian stock Telebrás.

This paper is organized as follows. In Section 2, we describe the many empirical observation for the index S&P 500 and the Brazilian stock Telebrás. In Sections 3–5, we describe that these observations can be well reproduced by using the first Poincaré return time, a dynamical variable, to simulate the returns. In Section 6, we present the conclusions of this work.

2. Data analysis

This paper shows and explain several empirical statistical manifestations observed in the stock market. These manifestations are: (i) The return distribution is a Poisson-like distribution; (ii) the return distribution functional form is preserved for long time periods, and therefore, it has a slow convergence to the Gaussian behavior; (iii) the asymptotic behavior of the return distribution follows a power law; (iv) the amplitude variation of the return with respect to time follows a typical scaling power law;

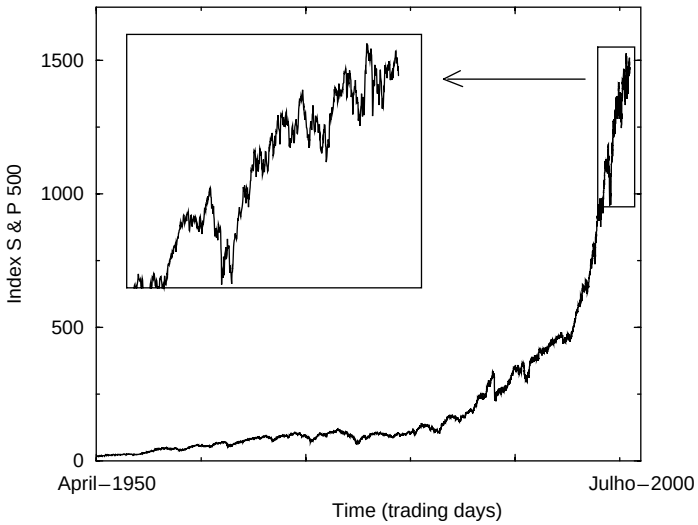

Fig. 1. (A) The closing daily S&P 500 index for a period from January of 1950 up to July 2000.

(v) there is a long persistence in the linear correlation function of the amplitude variation of the return (which is related to the volatility of the return); and (vi) the sign of the return changes with high uncertainty. In addition to explaining these empirical observations, in this work we also explain other empirical observations described in Refs. [7,8,11]: (vii) The distribution of the recurrent time is a Poisson distribution; (viii) the recurrent time follows a power law with respect to the size of the reference interval with characteristic exponent close to one (typical of super-diffusive systems); (ix) the average amplitude of the recurrent time with respect to time is a linear function; and (x) The average interval of time the return of the index takes to assume again the same value, within a reference interval δ, is inversely dependent on the δ, for smaller return values, and exponentially dependent (with exponent proportional to the return value) for higher return values.

Part of the data to be analyzed is shown in Fig. 1, where we show the trading daily evolution of the closing value of the S&P 500 index, $Y(t)$, for a period from January of 1950 to July 2000. This figure also shows a magnification of the small box indicated on it. We deal with $Y(n\Delta t)$, indicated by Y_n, where Δt is the sampling rate (in Fig. 1 $\Delta t = 1$ day).

The appropriate variable to analyze a stock index fluctuation is the return of Y_n:

$$R_n(\tau) = \frac{Y_{n+\tau} - Y_n}{Y_n}\,, \tag{1}$$

where the time interval τ represents the interval of time we want to analyze the fall/down of the index value, and $\tau \geqslant \Delta t$. Fig. 2 shows the values of R_n, corresponding to the Y_n shown in the magnification of Fig. 1.

Next, we show a few properties of the data $R_n(\tau)$ which led us to our modeling of the stock index, as well as modeling of any financial stock.

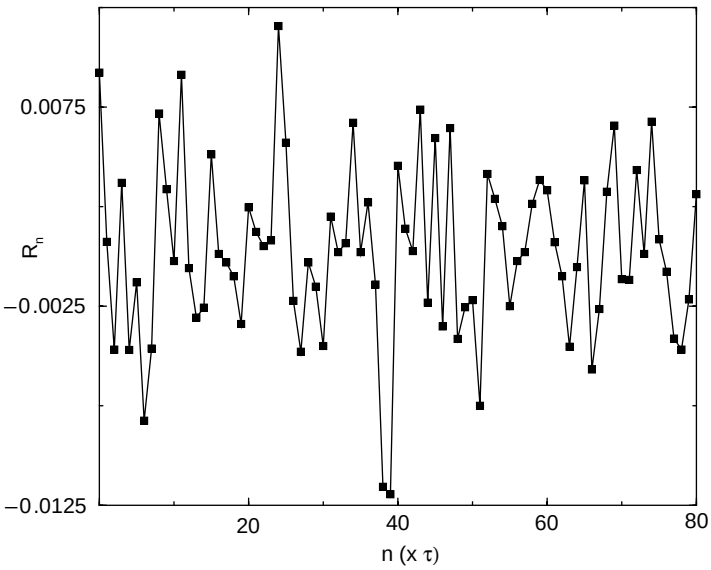

Fig. 2. A sample of the return of the data within the small box in Fig. 1.

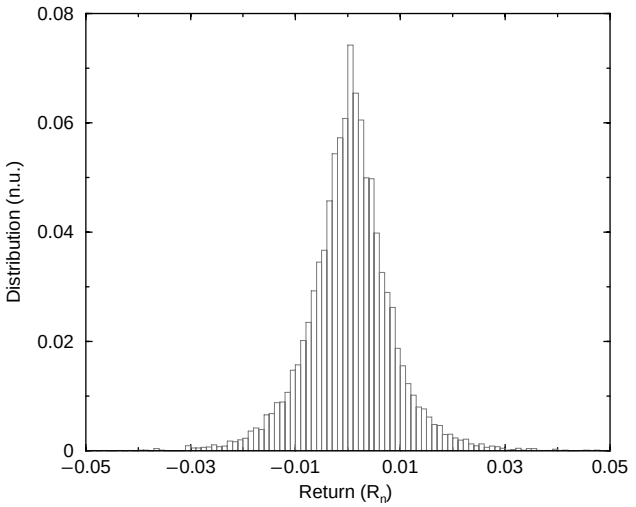

Fig. 3. Distribution of the return, defined in Eq. (1), of the S&P 500 index.

Fig. 3 shows the distribution $\rho(R_n)$ of the data shown in Fig. 1. This result can be described by a convolution of two Poisson distributions (property (i)). For $R_n > 0$, $\rho[R_n(\tau)]=\sigma \exp-(R_n/\langle R_n^+\rangle)$ and for $R_n < 0$, $\rho[R_n(\tau)]=\sigma \exp(R_n/\langle R_n^+\rangle)$. The convolution

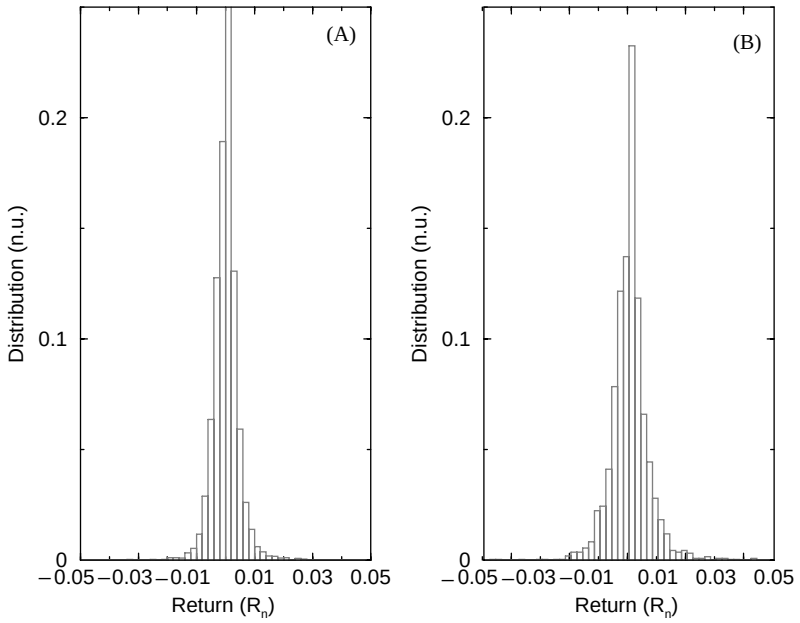

Fig. 4. Distribution of the return, defined in Eq. (1), of the Brazilian Stock Telebrás collected every 15 min (A) and collected every 30 min (B).

led us to

$$\rho[R_n(\tau)] = \sigma \exp - (|R_n - \langle R_n\rangle|/\langle R_n^+\rangle)\,, \tag{2}$$

where R_n^+ denotes values of R_n bigger than its average $\langle R_n\rangle$, and σ is proportional to $1/\langle R_n^+\rangle$. Assigning σ to be equal to $\frac{1}{2}\langle R_n^+\rangle$, Eq. (2) represents the probability distribution of the $R_n[(\tau)]$. In Fig. 3, $\langle R_n^+\rangle = 0.00592188011$, $\langle R_n\rangle = 0.000385249611$, and $\langle R_n^-\rangle = -0.00604495901$.

There are two important measurements of R_n. One is $\langle R_n\rangle$ (the tendency of the index), the average of the R_n's. The other is $\langle R_n^+\rangle$ (proportional to what is called volatility of the index), the average value of all the R_n's bigger than $\langle R_n\rangle$. These quantities define the observed Poisson-like distribution of the return. Therefore, the return standard deviation, sometimes given in the literature, is not a proper measure of the return because it describes not a Poisson-like distribution width but the width of a Gaussian distribution.

For the S&P 500, we verified that the distribution $\rho[R_n(\tau)]$ preserves its form for τ till about 7 days (property (ii)). In Ref. [6] it was shown that the same distribution preserves its form up to about 4 days.

In Fig. 4 we show, for the Brazilian Stock Telebrás, that its return distribution form is preserved for distributions of different sampling time of 15 and 30 min, with data covering the period from 12/02/1999 to 11/09/1999. Note that the distribution form is the same as the one in Fig. 3. For Fig. 4A (15 min) $\langle R_n\rangle \cong 0$, $\langle R_n^+\rangle = 0.00335$,

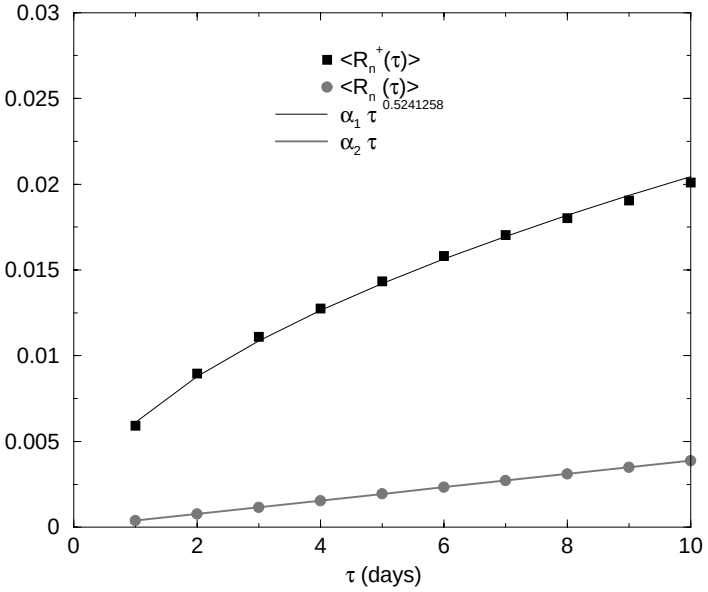

Fig. 5. Scaling power law for $\langle R_n^+(\tau)\rangle$ (squares) and $\langle R_n(\tau)\rangle$ (circles) with respect to τ. Lines represent fitting curves. Data of the S&P 500.

$\langle R_n^-\rangle = -0.00266$, and for Fig. 4B (30 min) $\langle R_n\rangle = 0.000121$, $\langle R_n^+\rangle = 0.00481$, $\langle R_n^-\rangle = -0.00411$.

We now show the variation of the return distribution with τ (iv), that is, the variations of the positive width $\langle R_n^+(\tau)\rangle$ and the average $\langle R_n(\tau)\rangle$ with τ. Thus, in Fig. 5 (for the S&P 500) we show in squares $\langle R_n^+(\tau)\rangle$, and in circles $\langle R_n(\tau)\rangle$. The lines are the fitted power-scaling laws

$$\langle R_n^+\rangle(\tau) = \alpha_1 \tau^{\beta_1}\,, \tag{3}$$

$$\langle R_n\rangle(\tau) = \alpha_2 \tau\,, \tag{4}$$

where $\alpha_1 = 0.00612$, $\beta_1 = 0.524$, $\alpha_2 = 0.000393$. We note that while $\langle R_n^+\rangle$ grows following a random walk criteria (once $\beta_1 \approx 0.5$), $\langle R_n\rangle$ changes linearly with τ. For the data of the Brazilian stock Telebrás with $\tau = 15$ min we obtained $\beta_1 \approx 0.55$.

To show the long persistence in the linear correlation function of the amplitude variation of the return, we introduce the variations of the distribution $\rho(R_n)$. To determine these variations, we initially calculate the averages $\langle R_n\rangle$ and $\langle R_n^+\rangle$ on each window of length l (which corresponds to l data points), as we shift forward this window for a time interval τ. The evolution of these averages are represented by the variations $\widetilde{\langle R_n\rangle}$ and $\widetilde{\langle R_n^+\rangle}$, obtained in days for the S&P 500, and in minutes for the stock Telebrás.

In Figs. 6 and 7, we show the variations of $\widetilde{\langle R_n(l\tau)\rangle}$ and $\widetilde{\langle R_n^+(l\tau)\rangle}$, for the S&P 500 ($\Delta t = 1$ day) and for the Telebrás ($\Delta t = 15$ min), as the time τ increases. The averages are calculated over a window of $l = 400$ days.

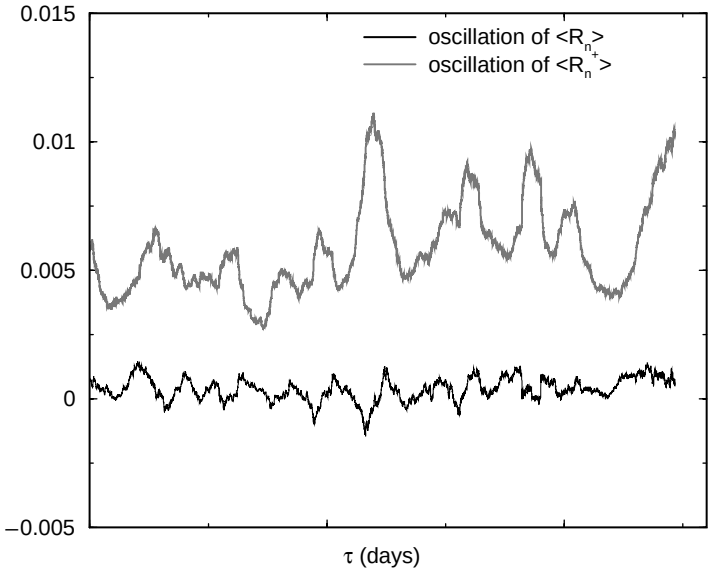

Fig. 6. Variations averages $\widetilde{\langle R_n \rangle}$ and $\widetilde{\langle R_n^+ \rangle}$, for the index S&P 500, calculated within a time window of 400τ, from 6 September of 1950 to 26 July of 2000.

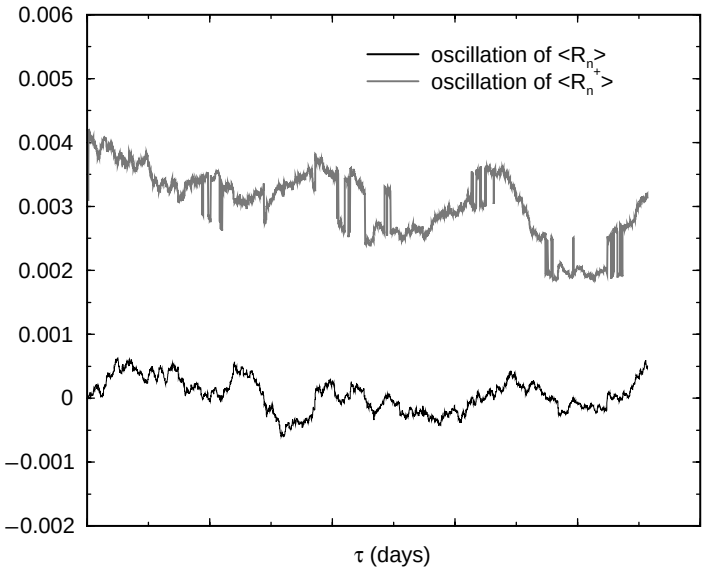

Fig. 7. Variations averages $\widetilde{\langle R_n \rangle}$ and $\widetilde{\langle R_n^+ \rangle}$, for the Brazilian stock Telebrás, calculated within a time window of 400τ, from 3 August of 1999 to 11 September 1999.

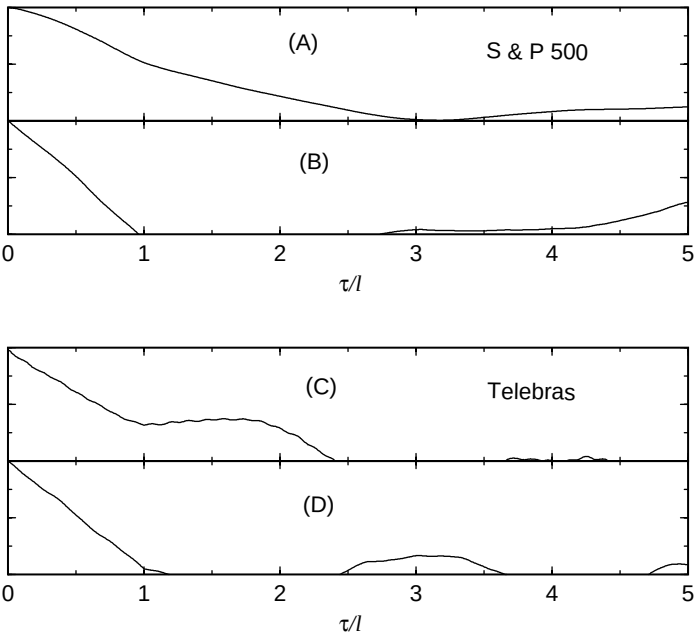

Fig. 8. Correlations of the variations of $\rho(R_n)$ with respect to $\delta t/l$ for the index S&P 500 (A,B) and the Brazilian stock Telebrás (C,D). (A,C) and (B,D) show the oscillations $\langle\widetilde{R_n^+}\rangle$ and $\langle\widetilde{R_n}\rangle$, respectively.

Now we calculate the linear correlation of the series shown in Figs. 6 and 7, using the following definition:

$$C(\tau) = \frac{\langle w(t+\tau)w(t)\rangle}{w(t)^2}\,, \tag{5}$$

where $w(t)$ represents the variations $\langle\widetilde{R_n(t)}\rangle$ or $\langle\widetilde{R_n^+(t)}\rangle$.

In Fig. 8(A) and (B), we show the linear correlation for the variations introduced above for the index S&P 500, and in Fig. 8(C) and (D) we show the same for the stock Telebrás with respect to τ/l.

We define the correlation time as the time δ_t, for which the correlation of $\langle\widetilde{R_n(t)}\rangle$ or $\langle\widetilde{R_n^+(t)}\rangle$ decays $1/e$. So, from Fig. 8, the correlation time of $\langle\widetilde{R_n^+(t)}\rangle$ is approximately equal to l while the correlation time of $\langle\widetilde{R_n(t)}\rangle$ is approximately equal to $l/2$. This shows that an analysis of data within a time interval l in the past is needed to have correlated data in the next l (or $l/2$ for $\langle R_n\rangle$) interval of time in the future. This result is important to define the time of observation needed in order to perform a useful prediction.

To demonstrate the high uncertainty of the sign of the return (property (vi)), we calculate the Shannon entropy [12] of the return of the index S&P 500.

Let $\mathscr{S} = \{s_0, s_1, \ldots, s_{2^k-1}\}$ be the 2^k sequences of k symbols, where each symbol represents either a positive or a negative return, and let $p_0, p_1, \ldots, p_{2^k-1}$ to be the probability of these 2^k sequences.

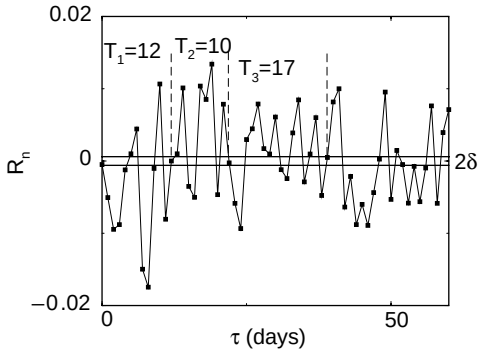

Fig. 9. The representation of the three return time T_n are indicated for an out-of-scale reference interval with width 2δ.

The uncertainty on the sign of the return is given by the Shannon entropy [12]

$$H_s = \frac{\sum_{j=0}^{j=2^k-1} p_j \log_2(1/p_j)}{2^k} . \tag{6}$$

In this equation, the unit of the entropy is in bits. Also, $0 \leqslant H_s \leqslant 1$. If $H_s = 1$, the uncertainty is maximum, and, therefore, the sign changing of the return seems random.

We find that the Shannon entropy of the return for the index is $H_s \cong 0.98$, a value very close to one; therefore, the sign of the return is very uncertain. However, the reason for which this entropy is not exactly 1, is the fact that the return has a tendency, that is, $\langle R_n \rangle > 0$. In the next section, we show that a return modeled by a dynamical system also have $H_s \cong 1$ for its sign.

To show that the distribution of the recurrent time is a Poisson distribution (property (vii)), we analyze the time of the return, T_n, for which R_n reaches a reference interval $I = [-\delta, \delta]$. In Fig. 9, we show a schematic representation on how we measure the series of T_n (for $\delta = 0.0006$) for the S&P 500 index.

The probability distribution of T_n, obtained for $\delta = 0.001$, $\rho(T_n)$, which can be seen in Fig. 10, is a Poisson distribution given by

$$\rho[T_n] = \mu e^{-\mu T_n} \tag{7}$$

with $\mu = 0.165$.

We find a scaling-power law relating the average value $\langle T_n \rangle$ with the reference interval half-width δ, observation (viii), given by

$$\langle T_n \rangle \propto \delta^{-\alpha} \tag{8}$$

with $\alpha = 1.09$, as can be seen from Fig. 11.

To show that the average time for which the return takes to come back q times to the reference interval is a linear function with respect to q (property (ix)), we construct a set W_n, with elements representing the sum of q subsequent elements of T_n, i.e.,

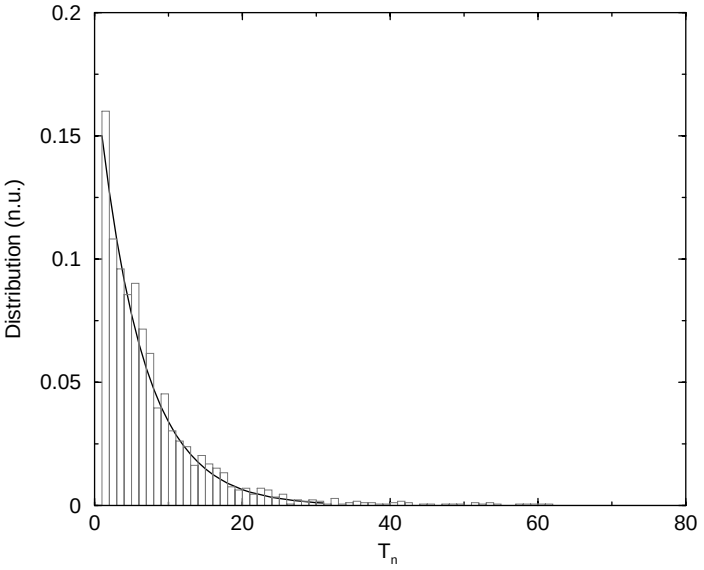

Fig. 10. Distribution of recurrent time T_n for the experimental data shown in Fig. 1.

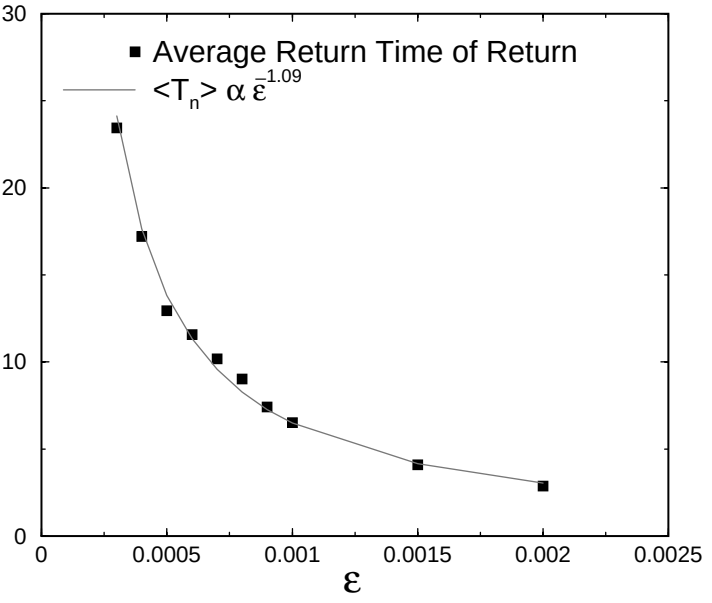

Fig. 11. Scaling power law for $\langle T_n \rangle$ (squares) with respect to ε. The line represents the fitted curve.

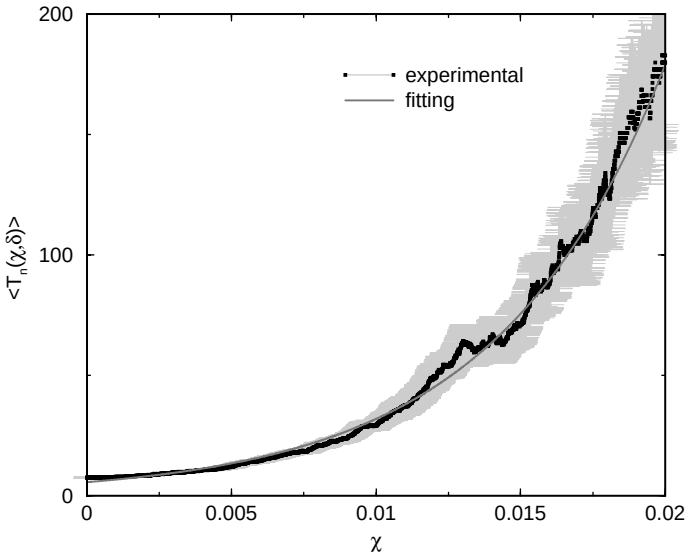

Fig. 12. The average recurrent time $\langle T_n(\chi,\delta)\rangle$ (dark curve) with respect to χ of the index S&P 500, and the exponential fitting curve (gray curve). The gray regions surrounding the experimental data represents the standard deviation of the average, $\delta = 0.001$.

$W_1 = T_1 + T_2 + \cdots + T_q$, $W_2 = T_{q+1} + T_{q+2} + \cdots + T_{2q}$, and so on. We obtain

$$\langle W_i(q)\rangle = q\langle T_n\rangle \,. \tag{9}$$

The last empirical observation (x) relates the time intervals with which rare events occur, in respect of the most likely events. Events here stand for some return value R_n in the interval $I(\chi) = [\chi - \delta, \chi + \delta]$. We call $\langle T_n(I)\rangle$ to represent the average of the time a return takes to leave and fall the interval $I(\chi)$. For the index S&P 500, we consider $\delta = 0.001$, and we find that

$$\langle T_n[I(\chi)]\rangle = \langle T_n[I(\chi = \langle R_n\rangle)]\rangle \exp^{\beta_e \chi} \,, \tag{10}$$

where β_e=5.707±0.002, and, γ=172.2±0.2. Note that $\langle R_n\rangle$=0.000385, and $\frac{1}{\beta}$=0.00581, a value very close to $R_n^+ = 0.00592$. As we will show further $\frac{1}{\beta_e} = \langle R_n^+\rangle$.

In Fig. 12, we show in small squares the experimental $\langle T_n(I)\rangle$ and, in the straight line, the fitting curve given by Eq. (10). We note in this figure that as we increase χ, the errors bars grow in size. This is due to the fact that, for higher χ, only a few recurrent times are obtained: the higher the χ the most unlikely the change of one to observe a return value within that interval.

If χ are small compared to δ, then, we find that $\langle T_n(\chi,\delta)\rangle \propto \frac{1}{\delta}$, a particular case of the one shown in Eq. (8).

In conclusion, the empirical observations of the stock market, discussed in this section, indicate the recurrent character of the analyzed oscillations.

3. Modeling distributions, power laws, and scalings

The task of modeling the stock market boils down to the task of modeling the return of an index, R_n, and the recurrent properties associated with the distribution of its values. In fact, the empirical properties described in the previous section appear naturally in measures of any chaotic dynamical system.

To model the stock market we look for a variable Q_n that is equivalent to R_n, i.e., presenting the same statistics, and scaling properties verified in the stock market oscillations. So,

$$\rho(R_n) = \rho(Q_n)\,. \tag{11}$$

This equation implies that the model for the discrete evolution of an index for a time interval τ is

$$Z_{n+1} = Z_n(1 + Q_n)\,. \tag{12}$$

Note that Eq. (12) is Eq. (1) for $R_n = Q_n$ and $Y_n = Z_n$.

Inspired by the empirical properties (i) and (vii), where the distribution of the returns is a Poisson-like, and distribution of the recurrent time is a Poisson, we conjecture that information given by the return R_n is equivalent to the one obtained from the recurrent time. In fact, we show that the return of the index can be modeled by the first Poincaré return time of a chaotic trajectory [7].

Thus, the proper type of system to model the return are the ergodic [13] ones, once all ergodic systems are recurrent. More than just ergodicity, to have a proper description of the dynamics of the market, we need another property from the type of recurrence needed, which is the assumption that the recurrence is created by the existence of many unstable periodic orbits. So, the ergodic system desired are the chaotic ones. Thus, to assure these properties, we model the return using the chaotic Logistic map [14,15],

$$x_{i+1} = 4.0x_i(1 - x_i)\,. \tag{13}$$

The relation between this chaotic dynamics and the variable Q_n (equivalent to the return R_n) is done through the Poincaré first return time $P_n(\varepsilon)$ of a chaotic trajectory, where $n = \{1, 2, \ldots, M\}$ is the number of times the trajectory of (13) falls in an x interval I of length ε, and P_n gives the time this trajectory takes to return to I. If x_0 belongs to I, and iterating (13) with x_0, the first point to fall in I is x_i, then the return time for $n = 1$ is $P_1 = i$. The representation of how this first Poincaré return time is computed can be seen in Fig. 13.

The Poincaré first return time, of the chaotic trajectory, measures the periods of the infinitely many unstable periodic orbits embed in the chaotic attractor. In other words, the Poincaré time measures how recurrent the dynamical system is. By proposing the description of a measure of the considered complex system by the use of this Poincaré time, we are taking into account the infinite periodic cycles that might exist in these complex systems.

In Fig. 14, we choose I as the interval $[0.100, 0.105]$, and the density distribution $\rho(P_n)$ is of the type

$$\rho[P_n(\varepsilon)] = \alpha_3 \mathrm{e}^{-P_n(\varepsilon)/\langle P_n(\varepsilon)\rangle}\,, \tag{14}$$

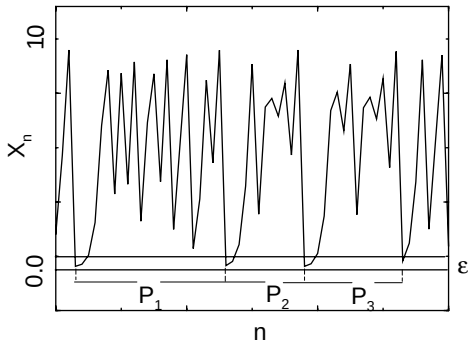

Fig. 13. Chaotic orbit for Eq. (13). The three first Poincaré return time are indicated for an out-of-scale interval ε.

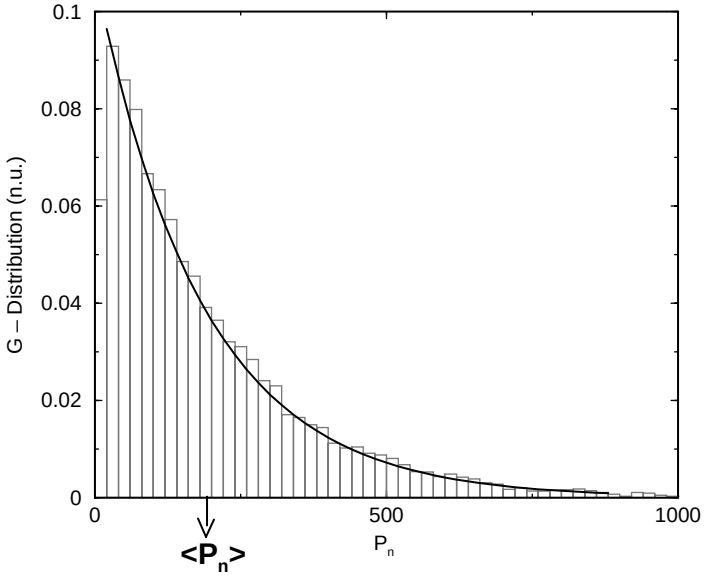

Fig. 14. Distribution of the Poincaré first return time for the chaotic trajectory of Eq. (13).

where α_3 can be rescaled to $1/\langle P_n\rangle$, such that (14) is a probability distribution. $\langle P_n\rangle$ is the average value of the series of P_n's. Note that this distribution of the first Poincaré return time [16,17] of the chaotic trajectory is a Poisson of the same type of the distribution for the recurrent time (Fig. 10).

For a specific interval length ε, the probability distribution $\rho(P_n)$ is obtained by the knowledge that the number of periodic orbits, embedded in the chaotic attractor, that pass through the interval length ε, with period lower than T, is $N(T) \approx \exp hT$, where h is the Kolmogorov–Sinai entropy (see Ref. [16]). Thus, following Ref. [16], we obtain the Poisson distribution given in Eq. (14).

The distribution $\rho(P_n)$ is a Poisson distribution while $\rho(R_n)$ is a Poisson-like distribution. In fact, $\rho(R_n)$ is the convolution of two Poisson functions, derived from a new variable Q_n, which is the subtraction of the two dynamically generated series P_n and P'_n:

$$Q_n(\varepsilon) = P_n(\varepsilon, x_0) - P_n(\varepsilon, x'_0)\,. \tag{15}$$

The convolution of $\rho[P_n(\varepsilon, x_0)]$ with $\rho[P_n(\varepsilon, x'_0)]$ is equal to $\rho[Q_n(\varepsilon)]$. Note that $\rho(Q_n)$ does not depend on either x_0 or x'_0, and that is a consequence of the fact that Eq. (13) has a ergodic trajectory, and thus, $\rho[P_n(\varepsilon, x'_0)] = \rho[P_n(\varepsilon, x_0)]$. We find that

$$\rho(Q_n) = \frac{\alpha_4}{2}\, \mathrm{e}^{\alpha_4 Q_n}\,, \tag{16}$$

where $\alpha_4 = 1/\langle P_n \rangle$, which means that the slope of this distribution is determined by $\langle P_n \rangle$. In fact, other characteristics of the Poisson of Eq. (14) are preserved in the distribution of Eq. (16).

Note that distribution (16) is of the same type of the distribution of the return of the index (Fig. 3), as well as the return of the Telebrás (Fig. 4).

One important characteristic of the distribution of Fig. 10, described by Eq. (14) is its asymptotic behavior. Due to the invariance in the characteristics of the Poisson and the Poisson-like distribution, the asymptotic behavior of the distribution of Fig. 10 is the same as the distributions of Figs. 3 and 4. So, to explain the decay of these distributions (property (ii)) we use a theoretical result [18], which states that

$$\rho(P_n) \sim P_n^{-\nu}, \quad P_n \to \infty\,, \tag{17}$$

where $\nu > 2$, which agrees with most of the empirical results about the power laws for the asymptotic behavior reported in Ref. [6].

There is also another important theoretical derivation which can explain the power-scaling law of the empirical distributions (iv).

It is stated in Ref. [18] that for an anomalous transport situation the moments of the displacement $r(t)$, of a particular chaotic system, can satisfy the asymptotic equation

$$\langle r(t) \rangle \sim t^{\mu/2}, \quad t \to \infty\,, \tag{18}$$

where $\mu = 2 - \nu$.

Assuming that the positive return $\langle R^+ \rangle$ has a diffusion power law of the type of Eq. (18) that describes diffusion of chaotic trajectories, we obtain

$$\langle R_n^+(\tau) \rangle \sim \tau^{\mu/2}, \quad \tau \to \infty\,. \tag{19}$$

Using the result of Ref. [6], for $\Delta > 1$ day, $\nu \cong 3$. So, for this case $\mu \cong -1$, and therefore,

$$\langle R_n^+(\tau) \rangle \sim \tau^{-0.5}\,, \tag{20}$$

similar to the result obtained for the index S&P 500 (Eq. (3)).

Eq. (19) can have different values for μ, depending on the recurrent time exponent ν, which also depends on the hidden dynamics. It is derived in Ref. [18] that $\mu = |\ln \lambda_S| / \ln \lambda_T$, where λ_S and λ_T are scaling parameters that characterize the fractal self-similarity of the space and time responsible to generate the observed recurrent times.

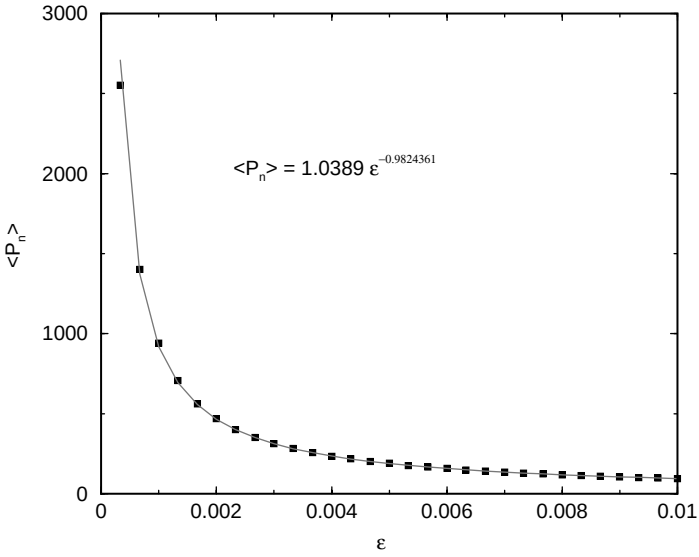

Fig. 15. Scaling of $\langle P_n \rangle$ with the interval $I = [0.100, 0.100 + \varepsilon]$.

These previous results agree with another empirical observation that the stock market has multi-scaling [9] and apparent multifractality [19,20].

To explain why the recurrent time follows a power law with respect to the size of the interval with characteristic exponent close to one (super diffusive type of power law for the recurrent time (viii)) we use another theoretical result. The scaling of $\langle P_n \rangle$ with ε does not only tell us about the width of its distribution, but it tell us about the fractal dimension of the hidden dynamical system involved. So, numerically, we find that

$$\langle P_n(\varepsilon) \rangle = \gamma \varepsilon^{-\sigma} , \tag{21}$$

where $\gamma = 1.039$ and $\sigma = 0.992$, values obtained by the fitting of the squared-shaped points in Fig. 15.

This preceding result can be obtained through the following derivations. Let M be a metric space and f the function (13), for which $f : M \to M$. Assume M is minimal, i.e., it is invariant, and does not contain another closed invariant subset. Let U be an open set of the set M, and μ the invariant measure of M. Thanks to Kac's Lemma [21,22], the average first Poincaré return time can be given by

$$\langle P_n \rangle = \frac{\mu(M)}{\mu(U)} , \tag{22}$$

where $\mu(M)$ can be set to be equal to one.

Assuming that the open set U is simply an interval $B[\varepsilon]$ of size ε[1] on M, and using the result of [23]

$$\mu(B[\varepsilon]) \propto \varepsilon^{D_p} , \tag{23}$$

where D_p is the pointwise dimension, which for almost every x on M is equal to the fractal dimension D_0. Therefore, using Eqs. (22) and (23), we can say that

$$\langle P_n \rangle \propto \varepsilon^{-D_0} , \tag{24}$$

what agrees with Eq. (21), by doing $D_0 = \sigma$.

In order to have the characteristics of $\rho(Q_n)$ exactly as $\rho(R_n)$, we rescale Q_n as

$$Q_n = [aP_n - bP_{n+1}]/F , \tag{25}$$

where $a - b$ represent the shift of the distribution on $Q_n = 0$ and F is a scaling factor. We choose a, b, and F to satisfy $\rho(R_n) = \rho(Q_n)$ and $\langle R_n^+ \rangle = \langle Q_n^+ \rangle$ (Q_n^+ is the average of the Q_n's that are bigger than $\langle Q_n \rangle$), and analyzing m values of the return $R_n(\tau)$, we obtain

$$F(\tau, \varepsilon) = \frac{\langle P_n(\varepsilon) \rangle}{\langle R_n^+(\tau) \rangle} , \tag{26}$$

$$b(\tau, \varepsilon) = \frac{F \langle R_n^-(\tau) \rangle \langle R_n^+(\varepsilon) \rangle}{\langle P_n(\varepsilon) \rangle (\langle R_n^-(\tau) \rangle - \langle R_n(\tau) \rangle)} , \tag{27}$$

$$a = b \left(1.0 - \frac{\langle R_n(\tau) \rangle}{\langle R_n^-(\tau) \rangle} \right) = 1.0 , \tag{28}$$

where $\langle R_n^+ \rangle$, $\langle R_n^- \rangle$, and $\langle R_n \rangle$ are the average values calculated for an assembling of m successive values, where R_n^- are the values of R_n smaller than $\langle R_n \rangle$. $\langle P_n \rangle$ is given by Eq. (21). Every solution of Eq. (25) is supposed to produce values with the same sampling of the stock data that Eq. (25) is simulating. Therefore, it is reasonable to say that one iteration of Eq. (25) corresponds to a unit time interval of Eq. (1).

To obtain Eqs. (28) and (26) we use the fact that ergodicity implies that $\langle P_n(\varepsilon, x_0) \rangle = \langle P_n(\varepsilon, x_0') \rangle = \langle P_{n+1}(\varepsilon, x_0') \rangle$. To speed up calculations we use the series $\langle P_n(\varepsilon, x_0') \rangle$ and $\langle P_{n+1}(\varepsilon, x_0') \rangle$ in Eq. (25), which are both generated by the same initial condition. In fact, the series P_{n+1} is a shift of P_n.

In Fig. 16 we show the distribution $\rho(Q_n)$, for the parameters $F = 32052.354$ and $b = 0.940$, calculated using the data of Fig. 1. For this figure, $\langle Q_n^+ \rangle = 0.00577$ ($\langle R_n^+ \rangle = 0.00592$), $\langle Q_n \rangle = 0.000361$ ($\langle R_n \rangle = 0.000385$), and $\langle Q_n^- \rangle = -0.00536$ ($\langle R_n^- \rangle = -0.00604$).

Next, we want to explain the changing of $\langle Q_n^+ \rangle$ with respect to τ, i.e., $\widetilde{\langle Q_n^+ \rangle}$.

According to the central limit theorem, the distribution of a random variable, for a high time, tends to a Gaussian. However, in the stock market, the convergence to a Gaussian is very slow, and actually can only be noticed for $\tau > 7$ days. Therefore, there is a preservation of the distribution functional form of the return for a long time (property (iii)), suggesting that the central limit theorem is not appropriate to fully describe the evolution of R_n distribution.

[1] Note that for D-dimensional system, $B[\varepsilon]$ is not an interval, but a D-dimensional ball on M.

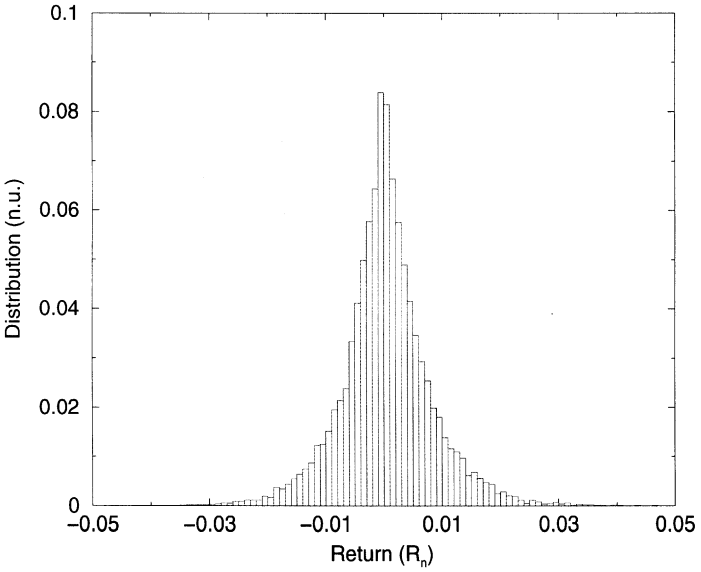

Fig. 16. Distribution of Q_n calculated from Eq. (25), for $F = 32052.3537$ and $b = 0.940087541$, simulating Fig. 3.

To discuss further this dynamical behavior of the stock return we present some additional properties of the Poincaré first return time.

The variable Q_n (that simulates the return), when calculated for the parameters F and b constants, presents the property (ix), as described by Eq. (9). To show that we define a variable W_n, which is the sum of Q_n's,

$$W_n = \sum_{i=0}^{k-1} Q_{n+i} \tag{29}$$

with the following property:

$$k\rho[Q_n] = \rho\left[\sum_{i=0}^{k-1} Q_{n+i}\right] , \tag{30}$$

where this equation means that the distribution $\rho[W_n]$ scales linearly with $\rho[Q_n]$.

In addition to this observation, both distributions, $\rho[Q_n]$ and $\rho[W_n]$, are Poisson-like. The distribution $\rho[\sum_{i=0}^{k-1} Q_{n+i}]$ describes the statistics of the simulated return for a time interval $k\tau$, and the distribution $\rho[Q_n]$ describes the statistics of the simulated return for a time interval τ. Thus, it is clear that the proposed model simulates data that have the same distribution form for different time intervals. This explains property (ii).

The long-range correlated variations, observed in both $\langle R_n \rangle$ and $\langle R_n^+ \rangle$ (Figs. 6 and 7), indicate that the parameters F and b should not be constants. Next, we show that

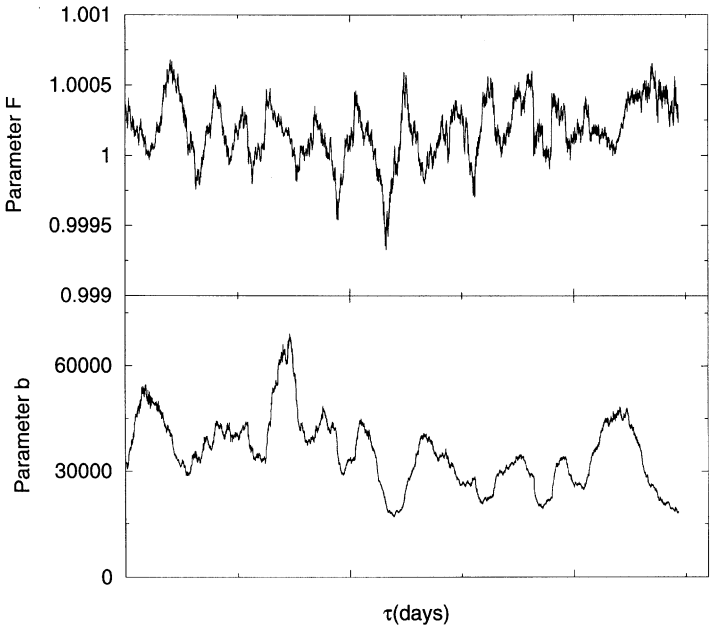

Fig. 17. Parameters b, and F (Eqs. (27) and (26), respectively), calculated for $\langle R_n \rangle$ and $\langle R_n^+ \rangle$ shown in Fig. 6, between 6 September of 1950 and 26 July of 2000.

these parameters, calculated through Q_n (solution of Eq. (25)), are not constant in time. In addition, we show that $\langle Q_n^+ \rangle$, and $\langle Q_n \rangle$ presents long-range correlated variations.

In addition to showing that $\langle \widetilde{Q_n^+} \rangle$ and $\langle \widetilde{Q_n} \rangle$ are long-range correlated, we want to clarify that the consequence of having $\langle \widetilde{R_n} \rangle$ and $\langle \widetilde{R_n^+} \rangle$ oscillating in a typical long-range correlated behavior is that the return with respect to the time τ follows the power-scaling law of Eq. (3). So, we calculate the parameters F and b, using $\langle \widetilde{R_n} \rangle$ and $\langle \widetilde{R_n^+} \rangle$, instead of $\langle R_n \rangle$ and $\langle R_n^+ \rangle$ in Eqs. (26) and (27). Parameters are adjusted to simulate the index S&P 500, and $\langle \widetilde{R_n} \rangle$, and $\langle \widetilde{R_n^+} \rangle$ are calculated using $l = 400$ data points in the past (an interval of 400 days). Fig. 17 shows the evolution of F and b for the analyzed data.

Using the parameters of Fig. 17, we calculate a series of Z_n using Eq. (25) into Eq. (12). Then, we show, Fig. 18 ($\alpha_6 = 0.0002$), that the average return and the positive average return of the predicted Z_n have the same type of oscillation of the index return, shown in Fig. 6. We also verify that the obtained Q_n^+ follows the same power-scaling law of Eq. (3). With this, we give an explanation of why Eq. (3) is found in the stock market. Therefore, it is very important that we understand better the oscillations of $\langle \widetilde{R_n} \rangle$ and $\langle \widetilde{R_n^+} \rangle$.

Now, we demonstrate that our model, by itself, generates variables Q_n, whose variations present long-range correlated oscillations. To do so, we calculate the parameters

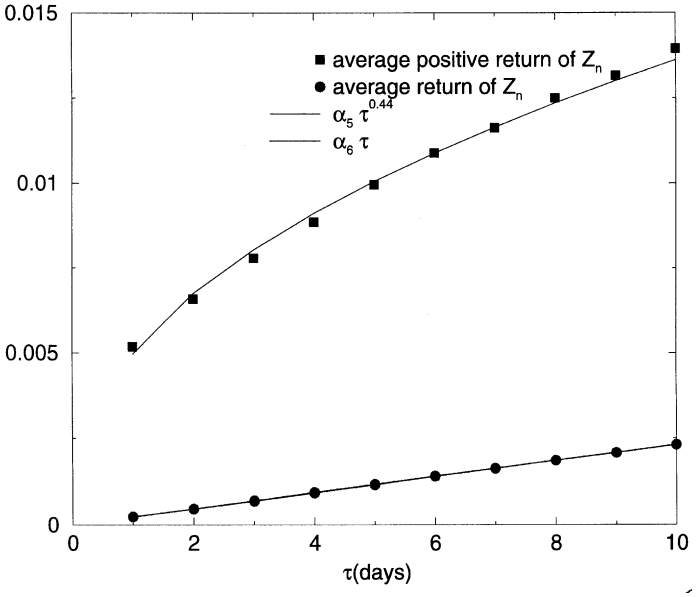

Fig. 18. The positive average return (squares) and the average return (circles) of the predicted Z_n. The positive average return follows a power scale law in respect of τ, with coefficient 0.44, and the average return follows a linear law.

F (Eq. (26)) and b (27), using also the predicted value Q_n. Initially, F and b are calculated using the return of $l = 150$ data points in the past. After performing one prediction, the next prediction is obtained for F and b, calculated using $l - 1$ data points in the past, and the predicted Q_1. The second prediction, is performed using F and b, calculated using $l - 2$ data points, and the predicted values of the return Q_1 and Q_2. This way, we generate a sequence of 5000 predictions, $Q_1, Q_2, \ldots, Q_{5000}$. In Fig. 19, we show the variations of the predicted Q_n, i.e., we show $\langle \widetilde{Q_n^+} \rangle$ and $\langle \widetilde{Q_n} \rangle$, using a window of $l = 400$. We see that the predicted return Q_n presents the same type of long-correlated oscillation present in Fig. 6.

For the simulated data of Fig. 16, we find that the Shannon entropy of Q_n is $H_s \cong 0.98$, a value very close to one; therefore, the sign of the return is very uncertain, exactly like described in the empirical property (vi).

4. Return and recurrent time equivalence

The observed equivalence of information contained in the return and in the recurrent time of the analyzed data can be explained using a fact about the type of observation realized in the system. The data can be collected using either M_t or M_s type of acquisition. We either set a sampling time, and then measure some quantity using this

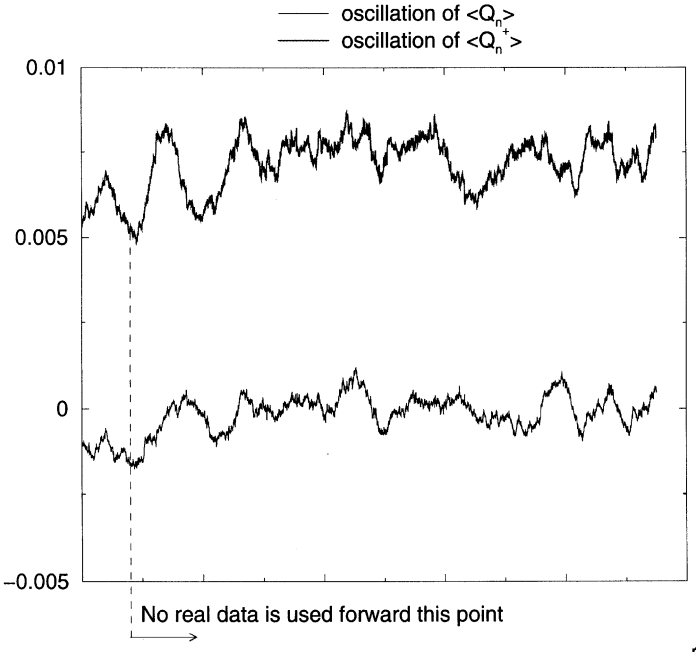

Fig. 19. Average variations $\widetilde{\langle R_n \rangle}$ and $\widetilde{\langle R_n^+ \rangle}$, for the predicted series Z_n, simulating the evolution of the index S&P 500.

time interval (M_t), or, we set some state we want to observe, and then measure the time the system takes to return to that state (M_s). The first kind of measurement is often the one used to make measurements. The second kind is frequently used when there is no way to make measurements of the first kind, as is the case for the spikes in neurons [24], the time interval between drops in the dropping faucet experiments [25], and heart beats [26].

Thus, a measure of type M_t, the return of the index (which is a measure of the downs and risings of the index) is equivalent to a measure of the type M_s, the recurrent time (that measure the time the return falls again within a given interval of values). The existence of such equivalence would eligible us to predict statistical properties of the average recurrent time, $\langle T_n \rangle$, by looking at the average of the return, $\langle R_n \rangle$, measured for a fixed time interval. And naturally, the vice versa of this previous affirmation is also true.

We define a measure of type M_t, in the dynamical system, the first Poincaré return time P_n. And the measure of type M_s is the finite time Lyapunov exponent defined as follows.

Before defining the chosen measure of type M_s, we first introduce a few concepts. We define the set $K = x_1, x_2, \ldots, x_q$ to be a trajectory of length q of Eq. (13), where x_1 can be almost every point on the set M. We define $\varsigma_N(x_i)$ (with N integer, $N \geqslant 1$, and $i = 1, \ldots, q$) to be the finite time Lyapunov exponent calculated along an N-step

length trajectory with the initial condition x_i. We call $\varsigma_N(x_i)$ as ς_N^i, which is defined by

$$\varsigma_N^i = \frac{1}{N}\sum_{j=0}^{N-1} \ln|G'(x_{i+j})|\,, \tag{31}$$

where G' is the derivative of Eq. (13), that is, $G' = 4(1-2x_i)$.

It was shown in Ref. [27] that if the set K is the interval $[0,1]$, the probability density of the finite Lyapunov exponents, $\rho(\varsigma_N)$, of this interval, is given by (we omit the index i because the distribution is calculated for all i's)

$$\rho(\varsigma_N) = \frac{N}{\pi}\,\frac{\exp^{-N|\varsigma_N-\Lambda|}}{[1-\exp^{-2N|\varsigma_N-\Lambda|}]^{1/2}}\,, \tag{32}$$

where Λ, the Lyapunov exponent of Eq. (13), can be obtained by Eq. (31) for $N\to\infty$.

Note that due to ergodicity (for high N), the probability density of Eq. (32) corresponds to the probability density of the finite time Lyapunov exponent, calculated over a length N trajectory.

While the Poincaré first return time is a spacial measure, and have its average value changed with respect to the size of the interval ε (according to the scaling-power law of Eq. (24)), the finite time Lyapunov exponent is a temporal measure and has its variance changed with respect to N, according to a power-scaling law of the type N^{-2} [27]. For more details in obtaining the distribution of finite time Lyapunov exponents see Ref. [28].

Assuming that the variable ς_N^i reflects the dynamics of the stock indexes, we expect that the return of the variable ς_N^i, defined by

$$S_i = \frac{\varsigma_N^{i+1} - \varsigma_N^i}{\varsigma_N^i} \tag{33}$$

is statistically equivalent to Q_n, i.e., equivalent to the return R_n of the S&P 500 index, shown in Fig. 3. And that is exactly what we verify, as shown in Fig. 20, done with the set K representing a trajectory of length $q = 5000$.

In dynamical system theory, the observed measurable should indicate local geometric properties of the phase space. Also, due to ergodicity, fixed sample time measurements taken on an interval of phase space, should reveal properties of the whole phase space. A way to measure a local geometric property of a system by a scalar measurable is by looking at the finite time Lyapunov exponent.

We are not going into details to study the dependence of the distribution $\rho(\varsigma_N)$ with respect to N. However, it is worthwhile to comment that while $\rho(P_n)$ depends on the fractal dimension, D_0 (Eq. (24)), $\rho(\varsigma_N)$ depends on the Lyapunov exponent Λ (Eq. (32)).

S_n and Q_n are equivalent, and thus, the statistic of Q_n should also be verified for S_n. Thus, demonstrating that the Poincaré first return time explains the empirical observations presented in the last section means that the measure ς_{N_i} also does. However, there are already many interesting theoretical results on the statistics of the Poincaré first return time based on dynamical properties of the chaotic system (as

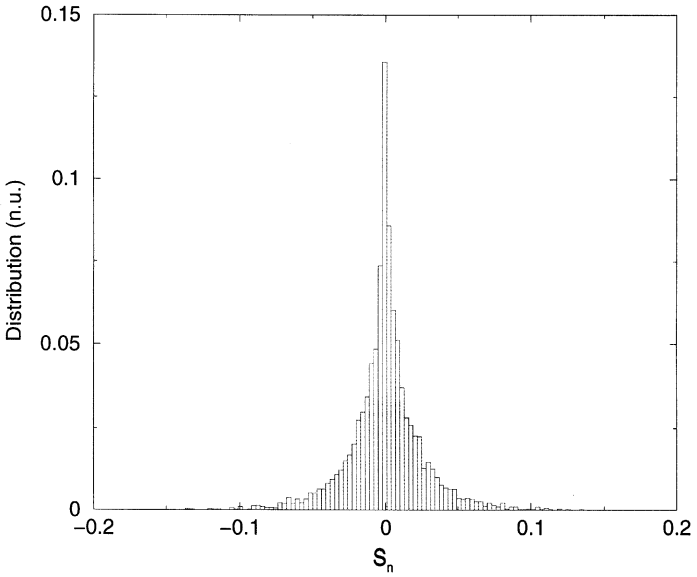

Fig. 20. Distribution of the return of the finite time Lyapunov exponent S_n, for $N = 50$, and $q = 5000$.

existence of unstable periodic orbits, and fractal dimension). Therefore, we prefer to continue working with the Poincaré first return time.

5. Stock index recurrence

We now derive the power law that relates the return time average, $\langle T_n \rangle$, with respect to the size of the reference interval used to obtain this average (property (viii)). For this case, as obtained in Eq. (21), we want to relate the average recurrent time of the simulated return Q_n to the interval $I(\chi = \langle Q_n \rangle) = [\chi - \delta, \chi + \delta]$ with respect to the interval δ. For that we use the fact that the probability distribution of the modeled return, Q_n, is a Poisson-like distribution as in Eq. (2). Thus, the probability, E, of finding a return within the interval I is given by

$$E[I(\chi = \langle Q_n \rangle)] = \int_{\langle Q_n \rangle - \delta}^{\langle Q_n \rangle + \delta} \frac{1}{2\langle Q_n^+ \rangle} \exp^{-|\chi + \langle Q_n \rangle|/\langle Q_n^+ \rangle} \, \mathrm{d}\chi \tag{34}$$

what results in

$$E[I(\chi = \langle Q_n \rangle)] = \tfrac{1}{2}(-\exp^{-\delta} + \exp^{\delta}) \, . \tag{35}$$

For small δ, we can approximate Eq. (35) by using $\exp^{\delta} \cong 1 + \delta$, and obtain

$$E[I(\chi = \langle Q_n \rangle)] \cong \frac{\delta}{\langle Q_n^+ \rangle} \, . \tag{36}$$

Once the probability E is found, the average recurrent time of the return is obtained by

$$\langle T_n[I]\rangle = \frac{1}{E[I]}\,. \tag{37}$$

Thus, applying Eq. (36) into Eq. (37), we obtain

$$\langle T_n[I(\chi = \langle Q_n\rangle)]\rangle \propto \frac{1}{\delta}\,, \tag{38}$$

as obtained experimentally (Eq. (8)).

Finally, we derive the relation between the average interval of time the return of the index takes to assume again the same value, within a time interval δ (x). In specific we want to relate rare events with likely events. The most likely event to occur is having the return of the index within the interval $I(\chi = \langle Q_n\rangle) = [\langle Q_n\rangle - \delta, \langle Q_n\rangle + \delta]$. We want to know an estimation of the time span, till we have again a return value falling in the interval given by $I(\chi) = [\chi - \delta, \chi + \delta]$.

As done previously, we just have to calculate the probability, $E[I(\chi)]$, with which the return falls in the interval I:

$$E[I(\chi)] = \int_{\chi-\delta}^{\chi+\delta} \frac{1}{2\langle Q_n^+\rangle} \exp^{-(|\chi+\langle Q_n\rangle|)/\langle Q_n^+\rangle}\,\mathrm{d}\chi \tag{39}$$

what results in

$$E[I(\chi)] = \frac{1}{2}\exp^{(-\chi+\langle Q_n\rangle)/\langle Q_n^+\rangle}[\exp^{\delta/\langle Q_n^+\rangle} - \exp^{-\delta/\langle Q_n^+\rangle}]\,. \tag{40}$$

Using Eq. (37), we obtain that

$$\langle T_n[I(\chi)]\rangle = 2\,\frac{\exp^{(\chi-\langle Q_n\rangle)/\langle Q_n^+\rangle}}{\exp^{\delta/\langle Q_n^+\rangle} - \exp^{-\delta/\langle Q_n^+\rangle}}\,. \tag{41}$$

A convenient form of working with Eq. (41) is using Eq. (35). Doing so, we obtain

$$\langle T_n[I(\chi)]\rangle = \langle T_n[I(\chi = \langle Q_n\rangle)]\rangle \exp^{\frac{(\chi-\langle Q_n\rangle)}{\langle Q_n^+\rangle}}\,. \tag{42}$$

Another simplification can be done in Eq. (42)

$$\langle T_n[I(\chi)]\rangle = \langle T_n(\chi = 0)\rangle \exp^{\chi/\langle Q_n^+\rangle}\,. \tag{43}$$

Note that Eqs. (42) and (43) are very similar, once $\langle Q_n\rangle$ is very small, and $\langle T_n(\chi = 0)\rangle \cong \langle T_n[I(\chi = \langle Q_n\rangle)]\rangle$.

To show that Eqs. (42) and (43) are correct, we use Eq. (25) to generate 100 000 values of Q_n, to simulate the return of the index S&P 500. Then, for $\delta = 0.0005$, we obtain that

$$\langle T_n[I(\chi)]\rangle = \sigma_T \exp^{\beta_T\chi}\,, \tag{44}$$

where $\sigma_T = 11.6530 \pm 0.0005$ and $\beta_T = 177.44 \pm 0.04$. Note that $1/\langle Q_n+\rangle = 173.34$, and $\langle T_n(\chi = \langle Q_n\rangle)\rangle = \sigma_T$.

In Fig. 21 we show in small squares the recurrent time, $\langle T_n(I)\rangle$, of the simulated return Q_n. The straight line is the fitting curve whose equation is shown in (10).

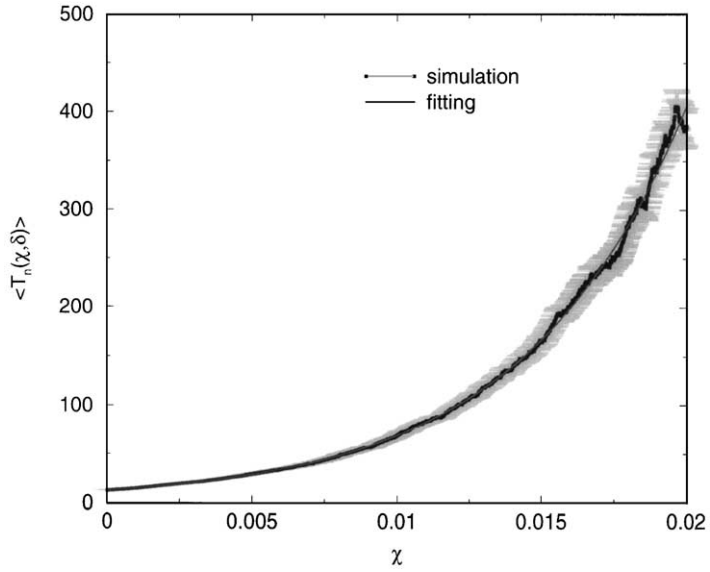

Fig. 21. The average recurrent time $\langle T_n(\chi,\delta)\rangle$ (dark curve) with respect to χ of the simulated return Q_n, and the exponential fitting curve (gray curve). The gray regions surrounding the experimental data represents the standard deviation of the average.

Different from what happens in Fig. 12, as χ increases the error bars do not grow too much. This is due to the fact that we used 100 000 values of Q_n, and thus, we have a better statistics.

6. Conclusions

We demonstrate that several empirical statistical evidences observed in the stock market are also present in the first Poincaré return time of a low-dimensional trajectory. Therefore, this dynamical measurement can be used as the basis of a model for the stock market return.

As important as describing the distribution of the return index R_n properly, there is a need to understand more the variations of the average quantities $\langle R_n\rangle$ and $\langle R_n^+\rangle$ with respect to the observation time τ. In case these variations are almost constant, $\langle R_n\rangle$ should scale with τ following a linear law, as described by Eq. (30).

We showed that there is an equivalence between the temporal measures, the return R_n, and spacial measures, the recurrent time of the return, T_n. This means information on the recurrent cycles of stocks in the stock market gives information on the volatility of this same stock, and vice versa. This equivalence was proven to exist in dynamical systems that are typically "fully" chaotic (as it is the case for Eq. (13)). For a system to be "fully" chaotic, there must exist a homoclinic or heteroclinic orbit in the surroundings of the chaotic set. Also, by "fully" one can think of a dynamics at

the chaos-stochastic border, where the dynamical system behaves either as a chaotic or as a stochastic system. Therefore, if this proposed model describes correctly the stock market dynamics, a stock fluctuation should have some statistical properties similar to those observed in randomic fluctuations.

We could relate the average time interval that we expect some return value to be observed with respect to the average return (volatility) of the index. This theoretical observation, also observed to happen in the stock market, guide us on how much time one should keep some stock in order to obtain some desired gain. This equation, in fact, can be seen as a test for the existence of properties in the data as observed in dynamically recurrent oscillation.

In Refs. [29,30] the common characteristics of the stock market oscillations with turbulence are proposed. We also found that the empirical observations (i,ii,iv,vii,viii,ix) described in this work are also present in edge turbulence of tokamak plasma [11]. Therefore, we believe the empirical properties, explained to be common of chaotic dynamical systems, could be seen as a set of characteristics to turbulence.

In Ref. [6] it is argued that the scaling behavior observed in the distribution of the returns may be connected to the slow decay of the volatility correlations. We do not disagree with this affirmation, but we prefer to emphasize that the scaling behavior is connected to the variations of the averages of the return (tendency) and the variation of the amplitude of the returns (volatility) with time.

One example of this is based on a peculiar observation regarding differences in the scaling laws of the average amplitude of the *recurrent time*, and the amplitude variation of the *return* with respect to time. The difference is that the recurrent time has a linear scaling law (very small linear correlation decay) and the return has a power-scaling law. This difference is due to the fact that the recurrent time is not affected by time variations of the averages of the return (tendency) and the variation of the amplitude of the returns (volatility) with time.

Any stock that verify the empirical properties described in this work should be a candidate to have its dynamics modeled by the proposed model. So, this model is not limited to a specific stock market of any country.

Acknowledgements

Part of the data used for this work was downloaded from the Website http://finance.yahoo.com/. This work is partially supported by FAPESP and CNPq. We also thank Ronaldo Castilho for the data of the Brazilian stock Telebras.

References

[1] L.J.B. Bachelier, Theory the la Speculation, Gauthier-Villars, Paris, 1900.
[2] B.B. Mandelbrot, J. Business 36 (1963) 394.
[3] R.N. Mantegna, H.E. Stanley, Nature 376 (1995) 46.
[4] R.N. Mantegna, H.E. Stanley, Phys. Rev. Lett. 73 (1994) 2946.
[5] R.N. Mantegna, H.E. Stanley, J. Stat. Phys. 89 (1997) 469.

[6] P. Gopikrishnan, V. Plerou, L.A. Nunes Amaral, Phys. Rev. E 60 (1999) 5305.
[7] M.S. Baptista, I.L. Caldas, Physica A 284 (2000) 348.
[8] M.S. Baptista, I.L. Caldas, M.S. Baptista, C.S. Baptista, A.A. Ferreira, M.V.A.P. Heller, Physica A 287 (2000) 91.
[9] J.-Ph. Bouchaud, Physica A 285 (2000) 18.
[10] H.E. Stanley, L.A.N. Amaral, D. Canning, P. Gopikrishnan, Y. Lee, Y. Liu, Physica A 269 (1999) 156.
[11] M.S. Baptista, I.L. Caldas, M.V.A.P. Heller, A.A. Ferreira, R.D. Bengtson, J. Stöckel, Recurrence on plasma edge turbulence, Phys. Plasmas 8 (2001) 4455.
[12] C.E. Shannon, W. Weaver, The Mathematical Theory of Communication, Bell system technical 27 (1948) 379.
[13] J. Guckenheimer, P. Holmes, Nonlinear Oscillations, Dynamical Systems, and Bifurcations of Vector Fields, Springer, New York, 1997.
[14] R.M. May, Nature 261 (1976) 459.
[15] D. Gulick, Encounters with Chaos, McGraw-Hill, New York, 1992.
[16] G.M. Zaslavsky, M.K. Tippett, Phys. Rev. Lett. 67 (1991) 3251.
[17] B. Saussol, Nonlinearity 14 (2001) 179.
[18] V. Afraimovich, G.M. Zaslavsky, Phys. Rev. E 55 (1997) 5418.
[19] J.-Ph. Bouchaud, M. Potters, M. Meyer, Eur. Phys. J. B 13 (2000) 595.
[20] B.B. Mandelbrot, Sci. Am. 280 (1999) 70.
[21] M. Kac, in: Probability and related topics in physical sciences, Lectures in Applied Mathematics, Interscience, London, 1957.
[22] I.P. Cornfeld, S.V. Fomin, Ya.G. Sinai, Ergodic Theory, Springer, Berlin, 1982.
[23] L.-S. Young, Ergodic Theory Dyn. Systems 2 (1982) 109.
[24] E.M. Izhikevich, Int. J. Bifur. Chaos 10 (2000) 1171.
[25] R.D. Pinto, W.M. Gonçalves, J.C. Sartorelli, I.L. Caldas, M.S. Baptista, Phys. Rev. E 58 (1998) 1.
[26] T.C. Chou, Electrocardiology in Clinical Practice, W.B. Saunders Co., Philadelphia, 1991.
[27] A. Prasad, R. Ramaswamy, Phys. Rev. E 60 (1999) 2761.
[28] R.S. Ellis, Entropy, Large Derivations and Statistical Mechanics, Springer, New York, 1985.
[29] S. Ghashghhaie, et al., Nature 381 (1996) 767.
[30] B. Holdom, Physica A 254 (1999) 569.